JOURNAL OF VIROLOGY, Dec. 1997, p. 9608–9617 Vol. 71, No. 12
0022-538X/97/$04.00+0

trans-Complementation of Yellow Fever Virus NS1 Reveals a Role in Early RNA Replication

BRETT D. LINDENBACH AND CHARLES M. RICE*

Department of Molecular Microbiology, Washington University School of Medicine, St. Louis, Missouri 63110-1093

Received 15 July 1997/Accepted 6 September 1997

Mutational analysis of the nonstructural protein 1 (NS1) of yellow fever virus (YF) has implicated it in viral RNA replication. To further explore this observation, we sought a method for uncoupling NS1 function from NS1 expression and processing as part of the large YF polyprotein. Here we describe a strategy for providing NS1 in *trans*, utilizing a noncytopathic Sindbis virus vector. Replication of a defective YF genome containing a large in-frame deletion of NS1 was dependent on functional expression of NS1. Recovered mutant virus was shown to contain the deletion and was neutralized by YF-specific antiserum. Complemented mutant virus increased in titer with kinetics similar to those of parental YF 17D but peaked at lower titers. *trans*-complementation has allowed us to derive high-titer, helper-free stocks of YF defective in NS1 with which to further characterize the role of this gene product in RNA replication. The first cycles of RNA replication were analyzed by using a sensitive strand-specific RNase protection assay. We document these events for mutant and wild-type viruses in the presence or absence of complementation. These data strongly suggest a role for NS1 prior to or at initial minus-strand synthesis.

Yellow fever virus (YF) is the prototype *Flavivirus*, a genus of enveloped, single-stranded, positive-sense RNA viruses which are typically transmitted via arthropod vectors and include such medically important pathogens as dengue, Japanese encephalitis, and tick-borne encephalitis viruses. Despite the development of an efficacious live attenuated YF vaccine (YF 17D) nearly 60 years ago, mosquito-borne yellow fever persists as a global public health problem of increasing proportions (25).

The YF genome is a single RNA molecule, approximately 11 kb in length, encoding one large open reading frame which is translated as a single polyprotein and processed into at least 10 discrete products by viral and cellular proteinases (reviewed in reference 33). The N-terminal region of the polyprotein produces virion structural components (C-prM-E); the remainder encodes nonstructural (NS) proteins (NS1-NS2A-NS2B-NS3-NS4A-NS4B-NS5). The principal function of NS proteins is replication of the viral genome, a process thought to occur in cytoplasmic complexes associated with cellular membranes. NS5 has homology to methyltransferases and RNA-dependent RNA polymerases (3, 31), and recombinant NS5 has recently been shown to contain this latter activity (40). The active site of the NS2B-3 serine protease localizes to the N terminus of NS3 (17, 32, 42), while helicase motifs are found in the C terminus of NS3 (18). This region of NS3 also seems to exhibit nucleoside triphosphatase and RNA triphosphatase activities in vitro (43, 44).

NS1 can be detected within infected cells, on the surface of cells, and it is efficiently secreted from cells. It is well conserved among flaviviruses (exhibiting 20 to 40% identity and 60 to 80% similarity), contains 12 conserved cysteines, and is singular among NS proteins for being glycosylated. YF NS1 is synthesized as a 352-amino-acid (aa) region of the polyprotein, inserted into the endoplasmic reticulum (ER) lumen via a signal sequence located at the C terminus of E which is presumably cleaved by host signal peptidase. Two N-linked glycans are rapidly added to NS1 in the ER (38), and at 10 to 20 min postsynthesis, NS1 is cleaved from NS2A (4). This cleavage event proceeds via an unknown mechanism involving an ER-resident host enzyme (9) and requires the eight C-terminal residues of NS1 as well as proximal sequences of NS2A (8, 30). Shortly after or concurrent with NS1-2A processing, NS1 exhibits increased hydrophobicity, associates with cellular membranes, and forms detergent-resistant, heat- and acid-labile homodimers (45, 46).

While no precise function has been ascribed to NS1, a role in viral RNA replication is emerging. NS1 appears to cosediment in sucrose gradients with heavy membrane fractions containing RNA-dependent RNA polymerase activity from Kunjin virus-infected cells (6). Furthermore, a YF genome containing a temperature-sensitive mutation in NS1 demonstrates a defect in RNA accumulation during growth under nonpermissive conditions (26). In addition, genomes containing lesions in the first or both N-linked glycosylation sites of NS1 were markedly impaired for RNA replication and growth in culture and exhibited decreased murine neurovirulence in vivo (27). Recently, immunolabeling of dengue 2 virus NS1 in cryoelectron micrographs localizes it within vesicular membrane structures that are associated with double-stranded RNA, presumably representing replicating viral RNA (23).

In this study we further our investigation into the role of NS1 in RNA replication by using a noncytopathic Sindbis virus (SIN) vector to express NS1. We describe the derivation of YF NS1-expressing cell populations by using SIN replicons, demonstrate that they are able to complement YF genomes containing a lethal deletion in NS1, and show that complementation depends on expression of NS1. This system has allowed us to derive stocks of mutant virus for investigation into the RNA phenotype of YF in the presence or absence of NS1. These experiments firmly establish a role for NS1 in the earliest stages of RNA replication.

* Corresponding author. Mailing address: Department of Molecular Microbiology, Washington University School of Medicine, 660 S. Euclid Ave., St. Louis, MO 63110-1093. Phone: (314) 362-2842. Fax: (314) 362-1232.

MATERIALS AND METHODS

Cell cultures, virus stocks, and plaque assays. BHK-21/J cells (kindly provided by Paul Olivo, Washington University) are a laboratory-passaged derivative of BHK-21 cells which exhibit increased contact inhibition and were found to be superior to BHK-21 cells obtained from the American Type Culture Collection for 3-day YF plaque assays. They are otherwise comparable to the parental cell in morphology, low-density growth, virus infectivities, and transfection efficiency. BHK cells and their derivatives were maintained in minimal essential medium (Life Technologies, Inc., Gaithersburg, Md.) containing 7.5% fetal calf serum and nonessential amino acids. High-titer virus stocks were derived by low-multiplicity passage (multiplicity of infection [MOI] of ≤0.1) in SW-13 cells or appropriate BHK populations for 42 to 48 h, clarified by centrifugation (3,000 × *g* for 10 min), aliquoted, and stored at −80°C. Virus stocks were titered by plaque assay essentially as described previously (34) except that overlays contained 0.75% agarose and plaques were allowed to develop for 60 to 72 h prior to formalin fixation and staining with crystal violet (1% [wt/vol] in 20% ethanol).

Plasmid constructions. Standard nucleic acid methodologies were used (1, 36). All constructions were verified by sequence and/or restriction analysis. pYFMΔSK and pYFMΔSP were assembled by T4 DNA ligase-mediated recircularization of blunt-ended (using T4 DNA polymerase), *Sac*I- and *Kpn*I-digested, or *Sac*I- and *Pvu*II-digested pYFM5.2 DNA (14, 34), respectively.

pSINrep19/NS1-2A contained aa 756 to 1355 of the published YF sequence (35). It was constructed by ligation of a 4,226-bp *Spe*I/*Stu*I fragment from pSINrep5/NS1-2A to 1,280-bp *Ssp*I/*Xho*I and 7,151-bp *Xho*I/*Spe*I fragments of pSINrep18 (11). pSINrep5/NS1-2A was constructed by subcloning a 1,811-bp *Xba*I fragment from pH2J1/sigNS1-2A (27) into the *Xba*I site of pSINrep5 (2). pSINrep19/NS1 (YF aa 756 to 1130) was constructed by first subcloning a 1,154-bp *Xba*I/*Spe*I fragment of pBSIISK−/sigNS1(−) into the *Xba*I site of pSINrep5. A 576-bp *Mlu*I fragment from pSINrep5/NS1 was then subcloned into pSINrep19/sigNS1-2A, replacing the 3′ end of NS1 and all of NS2A. pBSIISK−/NS1(−) (19) was generated by cloning a PCR amplification (forward primer 5′-CGGT CTAGAACATGACAATGTCCATGAGC-3′; reverse primer 5′-CCGTCTAG ATCAAGCTGTAACCCAGGAGCGCAC-3′) of YF cDNA into the *Xba*I site of pBSIISK− (Stratagene, La Jolla, Calif.).

SINrep21 derivatives containing NS1-2A and NS1 were constructed by subcloning from pSINrep19 by using common *Spe*I/*Bsp*120 and *Xba*I/*Bst*EII sites, respectively. pSINrep21/GFP was constructed by subcloning a red-shift variant, codon-optimized green fluorescent protein (GFP) gene (21) (kindly provided by Brian Seed, Harvard Medical School) into the *Xba*I and *Pml*I sites of pSINrep21.

An internal control for RNase protection, pGEM/GAPDH, was constructed by reverse transcription (RT)-PCR of the Syrian golden hamster glyceraldehyde-3-phosphate-dehydrogenase (GAPDH) gene from 1 μg of BHK-J RNA (forward primer 5′-GCTCTAGAGACGCAATGGTGAAG-3′; reverse primer 5′-CGAA TTCTTGCCATGGGTAGAG-3′) and cloning the 179-bp product into the *Xba*I and *Eco*RI sites of pGEM3Zf(−) (Promega, Madison, Wis.).

Full-length YF templates for transcription were assembled by using modifications of our previously described procedure (34). Essentially, *Aat*II/*Nsi*I fragments of pYF5′3′IV and pYFM5.2 were recovered from preparative low-melting-point agarose electrophoresis by phenol extraction. Full-length templates were constructed by ligation, *Xho*I digestion, and a second round of gel purification. This yielded templates for transcription of a single, full-length YF RNA species.

In vitro transcriptions. Runoff transcripts were generated in vitro, using T7 or SP6 RNA polymerase, depending on the promoter, as described previously (2, 26). Infectious YF and SINrep transcripts were synthesized in the presence of synthetic cap analog ^{m7}G(5′)ppp(5′)G (New England Biolabs, Beverly, Mass.). Nucleotide utilization was monitored by adsorption to DE-81 (Whatman) filter paper (36) and measuring incorporation of [5,6-^{3}H]UTP (in the case of viral transcripts, RNase protection assay [RPA] standards, and unlabeled RPA probes) or [α-^{32}P]CTP (for labeled RPA probes).

Transfections and selection of cell populations. Cells were prepared for transfection of viral or replicon RNAs as follows. BHK cells (or derivatives) were grown to 70 to 80% confluency in 150-mm-diameter dishes. Cells were harvested by trypsinization and washed three times in ice-cold RNase-free phosphate-buffered saline. Then 0.4 ml of a 2 × 10^7-cell/ml suspension were mixed with 5 to 10 μg of RNA, placed in a 2-mm gap cuvette (BTX Inc., San Diego, Calif.), and pulsed five times for 99 μs at 860 V in a model T820 electroporator (BTX). Following 10 min of recovery at room temperature, cells were returned to complete growth medium and plated. YF was allowed to grow for 42 to 60 h posttransfection prior to harvesting of the medium as described above.

DNA transfections were performed by using BES-buffered calcium phosphate (1) or cationic liposomes (1 μg of DNA and 8 μl of Lipofectamine [Life Technologies] per 35-mm-diameter dish of BHK cells [ca. 30% confluent]).

To select for replicon-containing cells, medium was changed to complete medium containing puromycin (5 μg/ml; Sigma, St. Louis, Mo.) at 12 h (for RNA) or 24 h (for DNA) posttransfection. Following selection (2 to 3 days), cells were passaged and maintained in medium containing puromycin. Experiments were performed with early (<7) passages of selected cell populations. It should also be noted that many experiments were performed in both SINrep19- and SINrep21-derived cell populations with similar results.

Protein analyses. For immunoprecipitation, cellular proteins were labeled in methionine- and cysteine-deficient Dulbecco's modified Eagle medium (Life Technologies) containing 2% fetal calf serum and Expre^{35}S^{35}S protein labeling mix (100 μCi/ml; NEN) for 3 h. Cells were lysed in 50 mM Tris (pH 7.5)–1 mM EDTA–0.5% sodium dodecyl sulfate (SDS) and clarified of insolubles by centrifugation (16,000 × *g*, 10 min). NS1 species were immunoprecipitated essentially as described previously (4), using monoclonal antibody 1A5 (37) and Pansorbin (Calbiochem, San Diego, Calif.).

RT-PCR. YFΔSK virus (1 ml; 10^6 PFU) was precipitated from medium by incubation with 4 ml of 40% (wt/vol) polyethylene glycol 8000 for 2 h at 4°C and pelleted at 14,000 × *g*, 4°C for 30 min. The pellet was resuspended in RNAzol, and the viral RNA was extracted, precipitated, and resuspended in 10 μl of H_2O. First-strand synthesis reaction mixtures contained 3 μl of viral RNA or YF in vitro transcripts and a YF genome-specific primer, using Moloney murine leukemia virus reverse transcriptase (New Englab Biolabs) at 37°C for 1 h. cDNAs were then amplified with KlenTaq LA DNA polymerase (Wayne Barnes, Washington University), using 25 cycles of 94°C for 30 s, 52°C for 30 s, and 72°C for 90 s.

Viral growth analyses. Cell populations were infected for 1 h at 37°C, washed three times with phosphate-buffered saline, and overlaid with complete medium. At indicated times postinfection, culture supernatants were sampled, clarified by centrifugation (14,000 × *g* for 5 min), and stored at −80°C until titrated by plaque assay. Detection limits were defined by the lowest dilution tested in the plaque assay.

Analysis of replicating viral RNA. RNA was isolated for RPA from cells by using Trizol (Life Technologies). Our RPA protocol used the same probes previously described (27) but has been optimized to enhance sensitivity. Parameters which were examined include specific activity and purity of riboprobes, RNA extraction procedures, hybridization kinetics, and digestion conditions. Briefly, upon homogenization, extracts were split into two equal parts for strand-specific analysis. Minus-strand analysis was based on the two-cycle procedure of Novak and Kirkegaard (28). Total cellular RNA (~10 μg) was hybridized overnight at 55°C in 30 μl [80% formamide, 40 mM piperazine-*N*,*N*′-bis(2-ethanesulfonic acid) (PIPES; pH 6.4), 400 mM NaCl, 1 mM EDTA] to an excess (10^{11} copies each) of unlabeled synthetic probes for minus-strand YF and BHK GAPDH. Samples were digested with RNase T_2 (23 U/ml; Life Technologies) for 1 h at 37°C, treated with proteinase K (37°C, 30 min), phenol extracted, and ethanol precipitated with 10 μg of yeast tRNA as carrier. Minus strands (secondary protection) or plus strands (primary protection) were detected by overnight hybridization to 5 pmol of labeled probes (synthetic plus strand or minus strand, respectively, and GAPDH) and RNase protection as described above. Products were resolved on 5% acrylamide–8 M urea–Tris-borate-EDTA gels and visualized with a phosphorimager (Bio-Rad, Richmond, Calif.) or by autoradiography. Undigested YF probes were 305 nucleotides (nt) in length, and protected fragments were 251 nt. Under conditions of RNase T_2 digestion, viral plus strands gave a slightly slower mobility, running at about 260 nt. Undigested and protected GAPDH probes were 199 and 167 nt, respectively. Labeled probes were synthesized by using [α-^{32}P]CTP (Amersham, Arlington Heights, Ill.) to a specific activity of 1.3 × 10^9 cpm/μg (YF probes) or 6.6 × 10^6 cpm/μg (GAPDH probe) and refined by RQ1 DNase treatment (Promega, Madison, Wis.), phenol extraction, preparative sequencing gel electrophoresis, reextraction with phenol, and ethanol precipitation. All probes were used within 2 days of synthesis. Strand-specific standards and unlabeled probes were prepared similarly to labeled probes except that reactions were spiked with trace amounts of [5,6-^{3}H]UTP to monitor nucleotide incorporation, yield, and RNA recovery. Following preparation and quantitation, these RNAs were aliquoted for single use and stored at −80°C. Standards were diluted in H_2O containing yeast tRNA (1 μg/μl), added to mock-infected BHK RNA during extraction, and processed in parallel with experimental samples except that GAPDH mRNA was not measured in standards reported here.

To quantitate replicating viral RNA species, band intensities of protected fragments were determined on a phosphorimager (Bio-Rad), using the manufacturer's software. Background (the comigrating region of mock-infected cell lane) was subtracted from experimental data, and data were normalized to GAPDH levels of mock-infected cells. Standard curves of input molecules versus pixel density were constructed based on dilution series of cold standards. In six independent standard curves constructed from four cold standard preparations, a linear relationship proved to be a good approximation of the data sets at 10^7 or more input molecules. However, the best-fit line did not accurately describe the lowest number of input molecules. We found that a better fit ($r^2 \geq 0.998$) was provided by a function of the form $y = m(x^n)$, where n was very close to 1, indicating a nearly linear relationship. This is likely due to a small unknown nonlinearity in the experimental system, perhaps due to phosphorimaging technology, pipetting error, etc. Because such power relationships were based on empirical observation within our assay, we feel that they are the most appropriate method for standard curve construction and regression analysis.

RESULTS

YF NS1 expression using SIN replicons. As tools to study NS1 function, we assembled derivatives of a noncytopathic SIN replicon for expressing NS1. Description of such vectors is

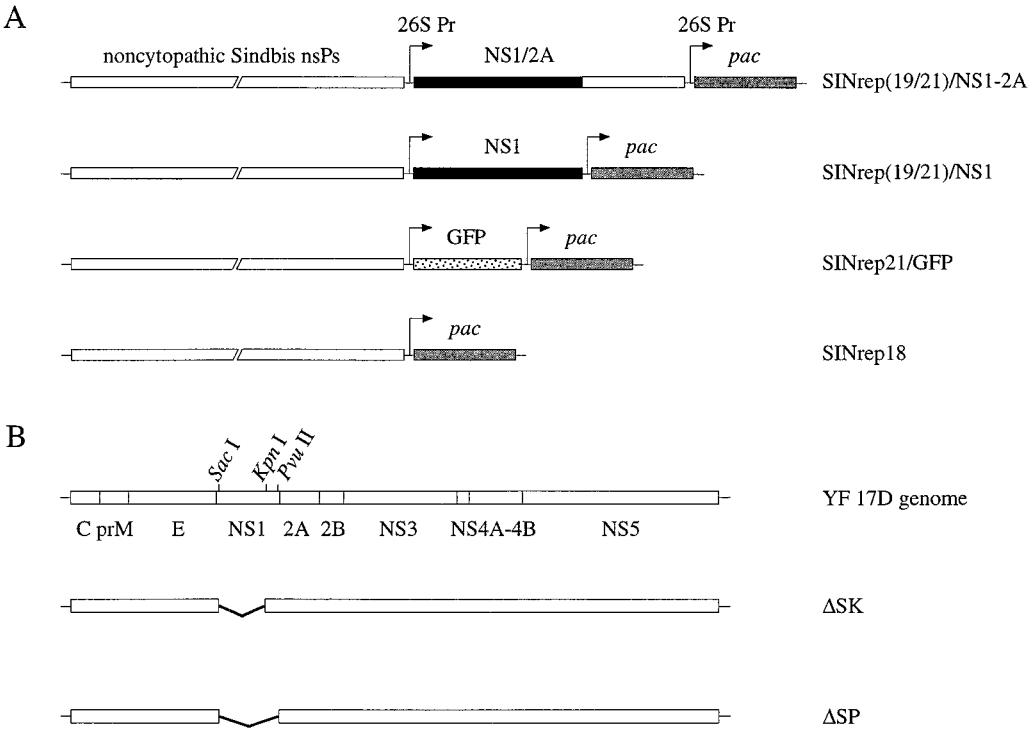

FIG. 1. Constructions used in this study. (A) Structures of replicon RNAs used in this study. Note that SINrep18 contained only a single subgenomic promoter. (B) Structure of the NS1-defective YF genomes. In-frame deletions were made in pYFM5.2 and used to generate infectious YF RNA.

forthcoming (10), but a useful review of SIN replicons, including a strategy for adapting them for persistent infection of BHK cells, has been published elsewhere (12). Briefly, SIN is the type *Alphavirus*, a distinct genus of enveloped, single-stranded, positive-sense RNA viruses (39). Recombinant self-replicating (replicon) SIN RNAs can be used to drive expression of heterologous genes in place of the SIN structural genes from a subgenomic promoter. Recently our lab has derived noncytopathic SIN replicons through puromycin selection of cells transfected with replicons expressing *pac*, the gene encoding puromycin *N*-acetyltransferase (11). These replicons are presumably maintained in the cytoplasm of cells and, because no SIN structural proteins are present, are propagated vertically through a population. SINrep19, a derivative of one such replicon (SINrep18), was found to be maintained in a cell population under puromycin selection and to be capable of long-term foreign gene expression from a second subgenomic promoter (10). Replicons may be launched via transfection of cells with SINrep19 RNA transcribed in vitro or transient transfection of cells with pSINrep21, a plasmid encoding the SINrep19 genome flanked by a Rous sarcoma virus long terminal repeat promoter and the Simian virus 40 polyadenylation signal (10).

The structures of four replicon RNAs used in these studies are illustrated in Fig. 1A. Because the role of NS2A in post-translational processing and function of NS1 is poorly understood, we decided to prepare expression constructs containing the NS1 region alone or NS1-2A region followed immediately by engineered stop codons. Constructs containing NS1 begin with the 24 C-terminal residues of E, which are believed to function as a signal for ER translocation and cleavage. Both RNA- and DNA-based vectors were prepared for each construct. We used the parental noncytopathic replicon, SINrep18, as a negative control for replicons launched via RNA transfection. A nonrelevant gene, encoding GFP, was also inserted into pSINrep21 to serve as a negative control for pSINrep21-derived replicons.

Following transfection, replicon-containing cell populations were selected with puromycin. Examination of NS1 protein expression is represented in Fig. 2. NS1 associated with YF-infected cells migrates as a doublet (ca. 41 and 44 kDa), which we have found to be due to partial or differential N-linked glycosylation (22, 26). Upon treatment with endoglycosidase H, the two forms coalesce into a single 40-kDa form (data not shown). NS1 species expressed via SINrep21 or SINrep19 closely resembled authentic NS1 in mobilities (lanes 3 and 4 and data not shown), and we therefore expect them to be similarly glycosylated. It appeared that in the absence of

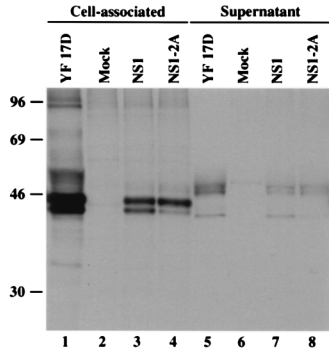

FIG. 2. NS1 protein expression. BHK-21 cells (mock infected or infected with YF 17D [MOI of 10] for 22 h) or BHK-SINrep21 derivatives were metabolically labeled. NS1 was immunoprecipitated from equivalent portions of cellular SDS extracts or labeling supernatant and resolved on an SDS–10% polyacrylamide gel. Sizes are indicated in kilodaltons.

TABLE 1. Recovery of infectious YF from RNA transcripts in BHK-SINrep19 populations

Cell type	Virus genotype	RNA specific infectivity (PFU/μg)[a]	Plaque titer (PFU/ml)[b]
BHK-SINrep18	17D	1.5×10^3	2.5×10^7
	ΔSK	≤50	≤10
	ΔSP	≤50	ND
BHK-SINrep19/NS1-2A	17D	7.0×10^2	2.5×10^7
	ΔSK	7.0×10^2	1.0×10^6
	ΔSP	≤50	ND

[a] Determined by plaque formation on BHK-SINrep19/NS1-2A.
[b] Plaque formation on indicated cells, using virus grown for 65 h on BHK-SINrep19/NS1-2A. ND, not determined.

NS1-2A cleavage, less NS1 was modified to the 44-kDa form (lane 3), perhaps due to increased ER retention time. Furthermore, NS1 was efficiently secreted from replicon-derived cells (lanes 7 and 8). These forms of NS1 also closely resembled YF-expressed NS1 (lane 5), which included a heterogeneous mixture modified with complex-type N-linked glycans (ca. 45 to 48 kDa) and a minor form (40 kDa) that is endoglycosidase H sensitive (22, 26). The quantity of this latter form seemed to correlate with the amount of the 44-kDa cellular form, suggesting perhaps a precursor-product relationship. In addition, replicon-expressed NS1 was found to form SDS-resistant, heat-sensitive homodimers in a manner identical to that for YF-expressed NS1 (data not shown). The expression of GFP was confirmed by fluorescence microscopy.

Replicon-expressed NS1 can function in *trans*. We next sought a functional assay in which to test replicon-expressed NS1. One method of analyzing gene function is to demonstrate complementation of a genome deficient in that gene. As NS1 has previously been shown to be required for YF replication (26), we define complementation as the ability to support the replication of a YF containing a defect in NS1. The following experiments take advantage of the fact that BHK-21 cells efficiently support replication of both SIN and YF. Initial experiments revealed no difference in YF plaquing efficiency on BHK-21 and BHK-SINrep19 populations (data not shown), indicating that YF and noncytopathic SIN replicons are compatible within the same host cell.

Previously in our genetic analysis of NS1, large deletions of the NS1 gene were engineered into our functional YF 17D cDNA clone via in-frame ligation (14). No YF was ever recovered from such deletion-bearing genomic RNA, suggesting a crucial role for NS1 in virus viability. We therefore chose two of these deletions (Fig. 1B) and tested whether they could be complemented in *trans* by replicon-expressed NS1. The residual NS1 gene of YFΔSK, which was deleted from the *Sac*I to *Kpn*I sites, retained the first 11 and last 81 codons and contained a novel Ala at the fusion site (260 codons removed). A larger deletion, YFΔSP, which extended from the *Sac*I to *Pvu*II sites, completely removed all of NS1 downstream of codon 11 and regenerated the C-terminal Ala immediately upstream of NS2A (340 codons removed). We reasoned that if replicon-expressed NS1 were able to complement the defects in NS1, defective YF should be infectious only to cells expressing NS1.

Full-length wild-type or defective YF genomes were synthesized and transfected into cells containing SINrep19/NS1-2A or SINrep18. A portion of these cells were then serially diluted and seeded onto fresh monolayers of BHK-SINrep19/NS1-2A for determination of RNA specific infectivity by infectious center assay. Following 3 days of incubation, plaques were visualized. As can be seen in Table 1, similar levels of infectivity were observed for wild-type RNA in both cell types. One mutant, ΔSK, initiated productive infection in BHK-SINrep19/NS1-2A but not BHK-SINrep18. Moreover, the specific infectivity of this RNA was identical to that of wild-type RNA. The other mutant, ΔSP, did not form plaques upon transfection of either cell type, perhaps due to the nature of the deletion (see Discussion). Virus present in the supernatant of ΔSK-transfected BHK-SINrep12/NS1-2A cells was amplified by one passage in these cells and then assayed for plaque formation on BHK-SINrep19/NS1-2A or BHK-SINrep18 cell populations. Again, ΔSK virus could be complemented only by BHK-SINrep19/NS1-2A; BHK-SINrep18 could not support ΔSK plaque formation either by RNA transfection or by infection with virus particles (Table 1). These data confirm that these deletions in NS1 are lethal for YF replication and also demonstrate that exogenous expression of NS1-2A can complement the ΔSK mutation in *trans*.

Typical plaques of YF 17D and ΔSK developed on SIN rep21-derived BHK populations are illustrated in Fig. 3. Plaquing efficiencies of YF 17D were similar in all three cell populations, suggesting that expression of additional NS1 or NS1-2A did not enhance or interfere with YF plaque formation. Untransfected BHK cells behaved identically to BHK-SINrep21/GFP cells (data not shown), indicating that GFP or the replicon itself was inert with regard to YF plaquing. We frequently observed slightly larger plaques in the presence of NS1 alone, although we have not ruled out the possibility that this size difference is due to subtle differences in cell density or growth during the course of the assay. ΔSK plaques developed on both the NS1- and NS1-2A-expressing cell populations, but not on the GFP control, confirming that NS1 expression is necessary for ΔSK growth. Aside from the larger plaque size on SINrep21/NS1 populations, ΔSK plaques resembled YF 17D plaques in size and morphology. These results indicate that NS1 expressed outside the context of NS2A is sufficient for ΔSK growth. Interestingly, ΔSK plaquing efficiency was consistently 10- to 20-fold greater on cells expressing NS1 than on those expressing NS1-2A. We also noted that upon repeated passage of BHK-SINrep21/NS1-2A populations (≥5 passages

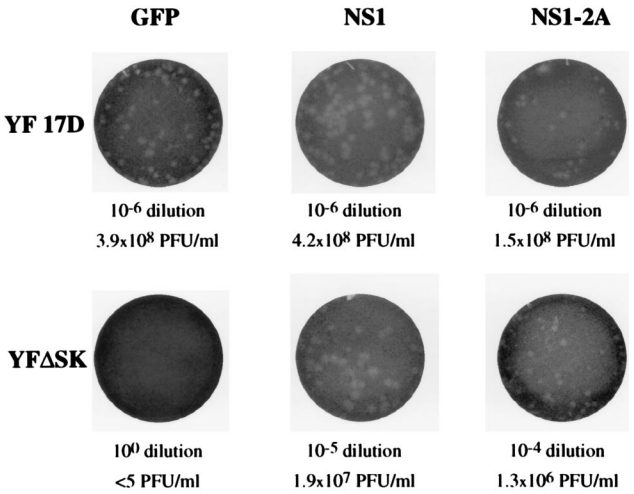

FIG. 3. Viral plaques. A total of 6×10^5 BHK-SINrep21 cells expressing GFP, NS1, or NS1-2A were seeded in 35-mm-diameter wells and infected with 0.2 ml of the indicated dilutions of high-titer-passaged virus stocks. After overlaying with agarose, plaques were allowed to develop for 60 h prior to fixation and staining. Images shown represent approximately 90% of the surface area of each well.

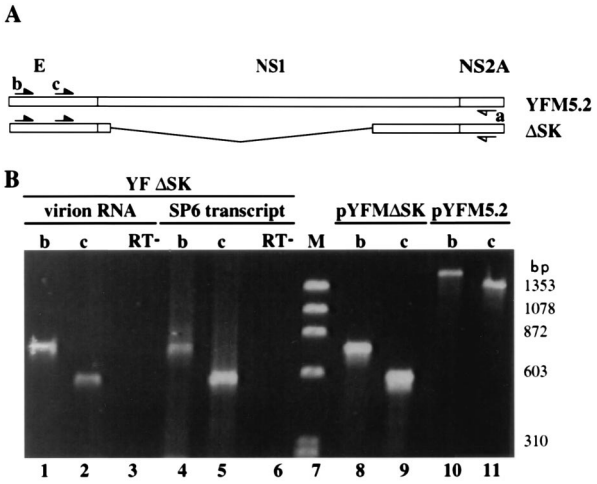

FIG. 4. YFΔSK viral RNA structure. (A) Arrangement of primers used in these experiments. (B) RNA isolated from YF ΔSK viruses (lanes 1 to 3) or in vitro synthesis (lanes 4 to 6) was primed for reverse transcription using a primer a. These cDNAs or plasmids pYFMΔSK (lanes 8 and 9) and pYFM5.2 (lanes 10 and 11) were amplified with primers a and b (lanes 1, 4, 8, and 10) or primers a and c (lanes 2, 3, 5, 6, 9, and 11). RT$^-$ reactions lacked reverse transcriptase; PCRs used primers a and c. M, *Hae*III digest of ϕX174 replicative-form DNA. The primers used correspond to the published YF plus-sense sequence (35): a = nt 3635 to 3616 (minus sense); b = nt 2288 to 2305 (plus sense); c = nt 2381 to 2401 (plus strand).

at 1:20), plaquing efficiency and plaque size of ΔSK decreased, while BHK-SINrep21/NS1 cells maintained their ΔSK plaquing efficiency over 10 cell passages. In all plaque assays tested ($n = 6$), ΔSK plaques were never observed on any cell type in the absence of cellular NS1 expression, even after three serial passages of virus, suggesting that revertant viruses were not produced.

We examined the specific neutralization of ΔSK PFU by using human vaccinee (YF 17D) serum. The numbers of YF 17D and ΔSK PFU could both be reduced approximately fivefold by incubating virus (24 h, 4°C) with a 1:640 dilution of heat-inactivated immune serum, while a 1:10 dilution of heat-inactivated preimmune serum had no effect on either virus. These data establish that ΔSK PFUs are indeed YF derived, and we therefore designate this virus YFΔSK.

Structure of YFΔSK virion RNA. To further characterize YFΔSK, we examined the structure of virion-associated RNA via RT-PCR analysis. Viral RNA was reverse transcribed by using a YF genome-specific primer and was amplified by using this primer and one of two opposing primers (Fig. 4A). The predicted products were 752 and 568 bp (primer pairs a-b and a-c, respectively) from YF ΔSK or 1,532 and 1,348 bp, respectively, from YF 17D. Reactions lacking reverse transcriptase were used to demonstrate that products were indeed derived from RNA. As seen in Fig. 4B, products of the expected sizes were obtained from YF ΔSK virion RNA, from in vitro transcripts used to generate this virus, and from the cloned cDNA template. YFΔSK virion RNA did not produce the products expected from wild-type virus (as seen in pYFM5.2 samples), suggesting that the defective YF genome is indeed reliably replicated. Furthermore, within the detection limits of this RT-PCR assay, no evidence of recombinant virus was seen. These results were corroborated by using a different reverse primer for cDNA synthesis and PCR (data not shown).

Growth of YFΔSK. The growth properties of mutant and wild-type viruses were examined on BHK cell populations by sampling virus culture supernatants over time and titrating accumulated virus via plaque formation on NS1-expressing populations. No differences were noted in YF 17D growth between BHK and BHK-SINrep21 derivatives, and expression of NS1, NS1-2A, or a nonrelevant gene product, GFP, also failed to show any effect on YF 17D growth (Fig. 5A). YFΔSK grew specifically on BHK-SINrep21/NS1 populations with kinetics resembling those of the parental virus, although YFΔSK failed to reach the same peak titer as YF 17D in three independent experiments (Fig. 5A and data not shown).

Since YFΔSK exhibited lower plaquing efficiency on NS1-2A-expressing cells than on NS1-expressing cells (Fig. 3), we compared the growth of this virus on these two cell populations. In addition, we compared the efficiency of complementation of the two vector systems, SINrep19 and SINrep21. As seen in Fig. 5B, expression of NS1 alone led to increased initial bursts of YFΔSK production, but by 36 h, both NS1 and NS1-2A populations accumulated similar levels of virus. These results were independent of the vector used to express NS1. These data suggest that expression of NS1 alone was more efficient at complementation early in infection. The lower peak titers in Fig. 5B than in Fig. 5A are likely due to the difference in plaquing efficiency between cell populations used as plaque substrates (Fig. 3), although this was not directly tested.

First-cycle analysis of YFΔSK and YF 17D RNA replication. We were particularly interested in using the high-titer mutant virus stocks made available by *trans*-complementation to examine the role of NS1 in RNA replication. Because YFΔSK stocks are apparently free of functional NS1 expression, we were able to examine the profile of RNA accumulation at early times postinfection in the presence or absence of NS1. For comparison, we examined the RNA accumulation of YF 17D under these same conditions. Unlabeled RNA probes were used as standards of RNA recovery and quantitation. In addition, as an internal control for RNA quality and quantity between samples, we examined the relative mRNA levels of a housekeeping gene, encoding GAPDH. No difference was observed in GAPDH mRNA levels in an initial experiment over a representative time course of YF infection.

Multiple parallel populations of BHK-SINrep21/GFP or BHK-SINrep21/NS1 cells (2×10^6/dish) were synchronously infected with YFΔSK or YF 17D at an MOI of 10. During adsorption, cells and virus were kept at 4°C to prevent internalization and uncoating (15). Following extensive washing in the cold, infections were initiated by addition of warm medium and equilibration to 37°C. At early times postinfection, total cellular RNA was isolated and split into two equal portions. One of these was used to examine minus-strand accumulation under conditions similar to those for the two-cycle RPA of Novak and Kirkegaard (28). Plus-strand accumulation was examined in the other portion of cellular RNA in a single-cycle assay.

The results of a representative minus-strand RNA analysis are shown in Fig. 6A. Lanes 2 through 5 illustrate our ability to recover and detect 10^6 input RNA molecules. At 10 min postinfection, only a very faint minus-strand signal could be detected over mock-infected cultures (lanes 6, 7, and 16). Minus strands accumulated over time in BHK-SINrep21/NS1 populations infected with YFΔSK (lanes 7 to 10) or BHK-SINrep21/NS1 (lanes 11 to 14) and BHK-SINrep21/GFP (lanes 21 to 24) populations infected with YF 17D. GFP-expressing cells failed to show appreciable minus-strand accumulation over the first 21 h of infection with YFΔSK (lanes 15 to 20). These profiles of minus-strand accumulation were reproduced in three separate experiments.

Similar analyses were performed a total of four times for viral plus strands, a representative example of which is illus-

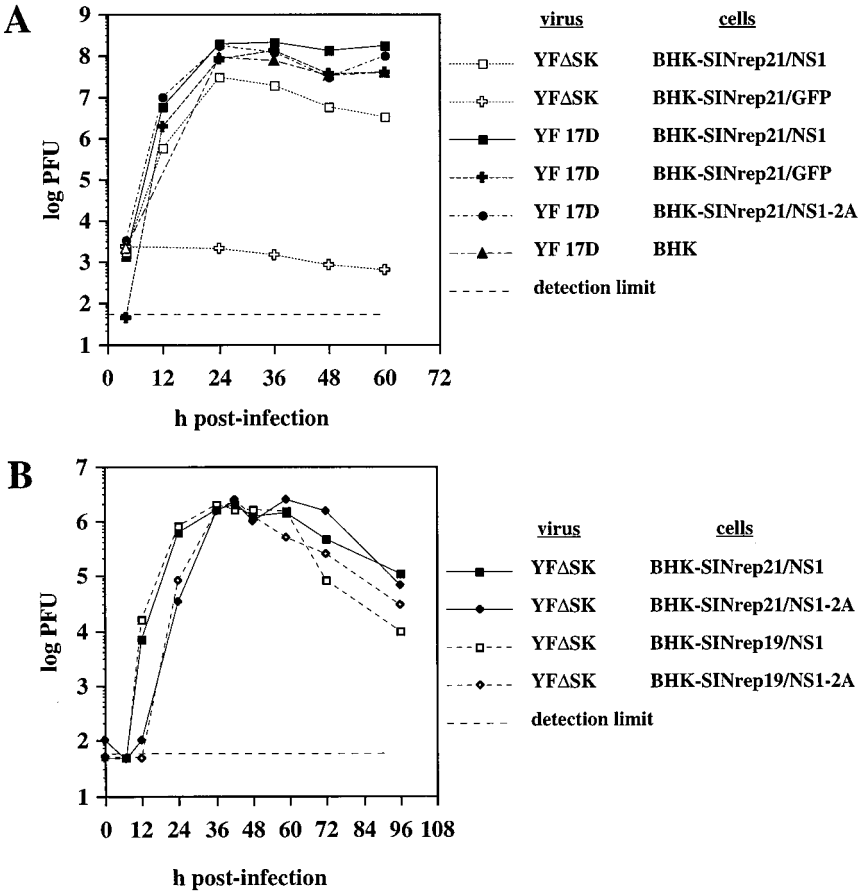

FIG. 5. Growth analysis of YF 17D and YFΔSK. (A) Indicated BHK or BHK-SINrep21 cells were infected in 60-mm-diameter dishes with YF 17D or YFΔSK (MOI of ≥10). Following sample collection (75 μl; 4, 12, 24, 36, 48, and 60 h), virus accumulation was monitored by plaque formation on BHK-SINrep21/NS1 cells. (B) Cells were infected in 35-mm-diameter dishes with YFΔSK (MOI of ~1). Samples (15 μl; 0, 6, 12, 24, 36, 42, 48, 60, 72, and 96 h) were titered by plaque formation on BHK-SINrep21/NS1-2A cells. This experiment was repeated once, with similar results.

trated in Fig. 6B. Large quantities of input plus strands, which are likely to be virion-delivered genomes, were seen at 10 min postinfection. Following a decline seen by 3 h, plus-strand levels rebounded for YFΔSK in BHK-SINrep21/NS1 cells (lanes 7 to 10) and for YF 17D in either cell population (lanes 11 to 14 and 21 to 24). Again, YFΔSK failed to show observable accumulation of viral RNA in the absence of NS1 expression.

Absolute quantities of viral RNAs were estimated by comparison to standards, as described in Materials and Methods. Accumulation of minus and plus strands from the experiment in Fig. 6 are plotted in Fig. 7A and 7B, respectively. Quantities which were derived from within the range of the standard curve are represented as closed points, while values outside this range (open points) were estimated by extrapolation and should be interpreted with caution. Nevertheless, several salient features are visible in Fig. 7. Minus-strand synthesis of wild-type virus appears to begin very soon after infection, since a minor increase is seen even by 3 h. Over the first 9 h, minus strands accumulated approximately 50- to 100-fold. In the presence of complementing NS1, YFΔSK demonstrated a similar increase in minus-strand accumulation over time. Importantly, in the absence of complementation, this virus failed to show a significant increase in minus strands, even by 21 h. A similar pattern was seen for viral plus strands. Following a decline in input plus-strand RNA, wild-type virus and complemented YFΔSK demonstrated an approximate 10-fold increase in plus strand from 6 to 9 h. Conversely, YFΔSK alone demonstrated only a decrease in viral plus strands. Results from similar experiments confirmed these observations.

DISCUSSION

Complementation is a particularly useful genetic tool for studying the function of obligately required genes. In this report, we describe the use of noncytopathic SIN replicons to deliver functional YF NS1 in *trans*. This expression system offers several advantages over traditional methods of foreign gene expression. Protein expression levels are reasonably high, the puromycin selection process is very rapid (days as opposed to weeks for G418 selection), and once selected, populations are remarkably easy to maintain. Because *pac* gene expression is linked to foreign gene expression, nearly every cell in a puromycin-resistant population expresses the gene of interest, obviating the need to clone individual cells. However, we remain cautious about the long-term expression of foreign genes since RNA viruses, including SIN, have high mutation rates. This problem is somewhat ameliorated by limiting studies to low passages of selected populations. Furthermore, introduction of replicons via DNA vectors improves expression stability (10), perhaps due to improved fidelity of eukaryotic RNA polymerase II over bacteriophage SP6 RNA polymerase.

It has recently been shown that SIN recombinants encoding the prM region of dengue 2 virus RNA interfere with replication of dengue 2 viruses in coinfected mosquito cells (13) and

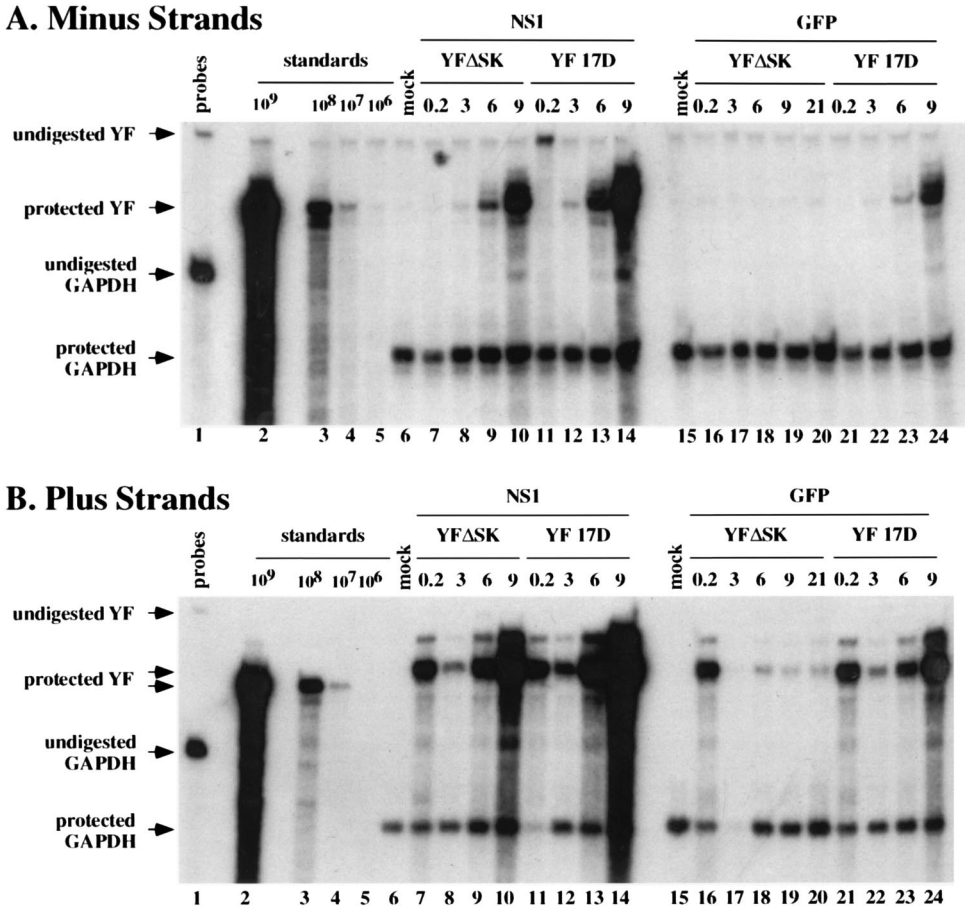

FIG. 6. RPA of viral minus and plus strands. RNAs were harvested at 10 min, 3 h, 6 h, 9 h, or 21 h postinfection. Equivalent portions of protected minus-strand (A) or plus-strand (B) reactions were subjected to denaturing electrophoresis and exposed to film for 12 h. Numbers above lanes 2 to 5 refer to number of input standard molecules; numbers above lanes 7 to 14 and 16 to 24 refer to hours postinfection. Lane 1 in both panels contained the equivalent of 10^{-4} μl of undigested minus strand (A) or plus-strand (B) probe and 0.1 μl of undigested GAPDH probe.

whole mosquitoes (29). The mechanism of interference is unknown but is postulated to operate through hybridization of SIN subgenomic RNAs encoding dengue 2 virus sequence to dengue 2 virus genomic plus- or minus-strand RNAs (13). In contrast, we observed no inhibition of YF 17D replication in cell populations expressing the YF NS1 or NS1-2A region via SINrep19 or SINrep21 (Fig. 3, 5A, and 7 and data not shown). These disparate results may arise from differences in SIN RNA levels between the two expression systems. SINrep18 accumulates much less viral RNA than parental SIN (11), and the hybridization model of Gaines et al. (13) predicts that interference should depend on the concentration of SIN RNA containing heterologous flavivirus sequences. In addition, the segregation of YF and SIN replication complexes may differ in mammalian versus arthropod cells, such that SIN RNA is less likely to interact with YF RNA. Alternatively, we cannot also exclude the possibility of differences between flaviviruses (YF versus dengue 2 virus) or the flavivirus genomic regions expressed (NS1 or NS1-2A versus prM). Nevertheless, no interference was observed in assays using the noncytopathic SIN replicon, making this an attractive system for future experimentation with flaviviruses.

Use of SINrep19 or SINrep21 led to NS1 expression that closely resembled authentic YF NS1 in glycosylation, secretion, and dimerization. Most significantly, replicon-expressed NS1 was shown to be functional for *trans*-complementation. This was demonstrated by the complete lack of detectable YFΔSK plaque formation, growth, and RNA replication in the absence of NS1 expression. Due to the prerequisite for cellular NS1 expression, we can exclude the occurrence of reversion in these experiments as well as the packaging of SIN replicons as helper viruses, perhaps within YF virions. We further conclude that the replication components of an unrelated RNA virus, SIN, cannot complement the defect in YFΔSK. Complemented mutant virus was shown to be neutralized by YF-specific serum and to retain the NS1 deletion. This virus also grew similarly to wild-type YF 17D although it did not reach as high a peak titer. This could be due in part to limiting amounts of NS1, particularly at late times of infection.

We did not observe complementation of a larger mutation, ΔSP. One possibility is the presence of a functional domain in the last 80 aa of NS1 that could not be complemented in *trans*. This would imply that the ΔSK mutation is not a complete null mutation although it has a severe phenotype. Alternatively, since the eight C-terminal residues of NS1 have been shown to be required for cleavage at the NS1/2A site (30), removal of these residues (as in ΔSP) is predicted to yield a fusion protein consisting of the first 11 aa of NS1 joined to NS2A. This could perturb the function of NS2A or the downstream processing of the YF polyprotein. Construction and complementation anal-

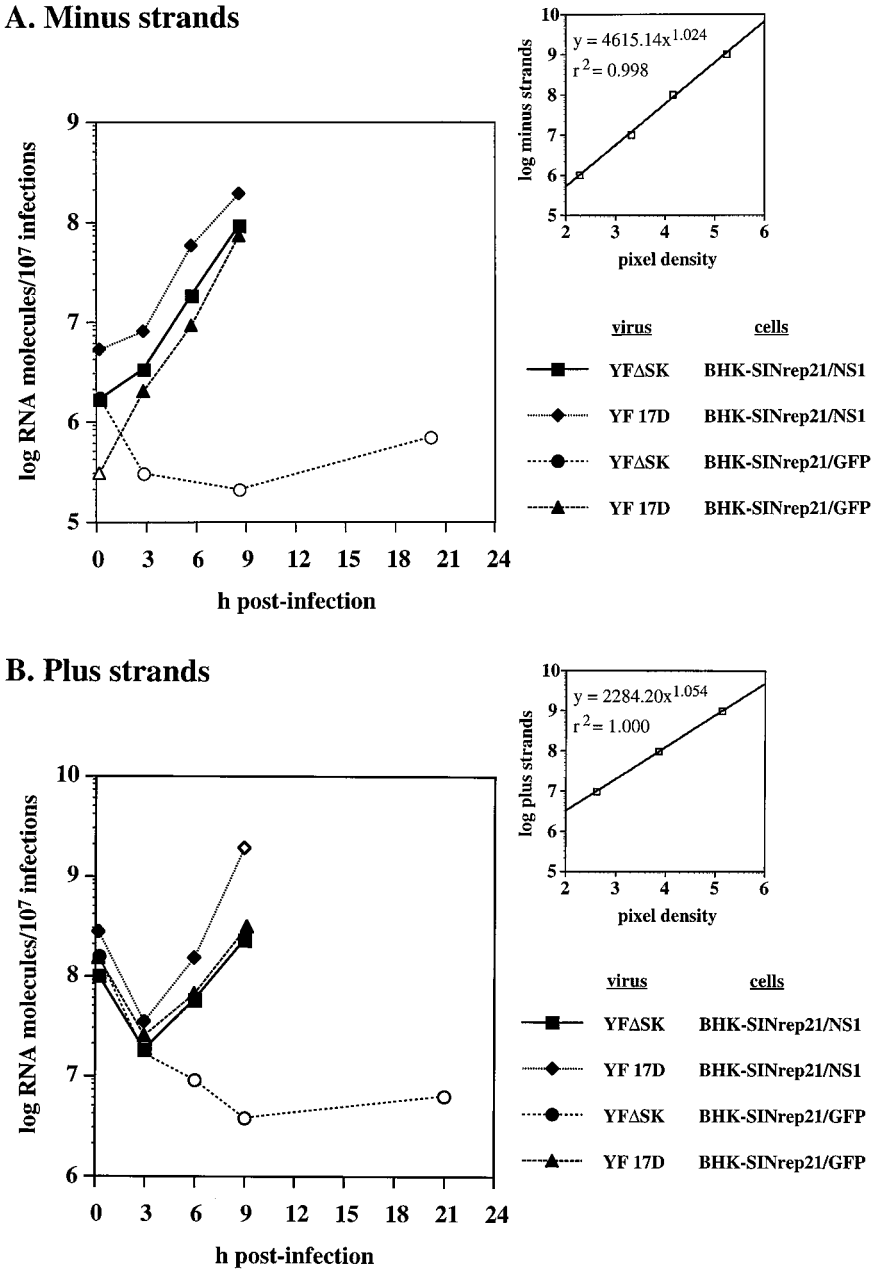

FIG. 7. RNA accumulation during the first replication cycles. Gels in Fig. 6 were scanned and quantitated as described in Materials and Methods. Results were plotted for minus-strand (A) or plus-strand (B) accumulation versus time. Closed points refer to values within the standard curve; open points were derived by extrapolation. Inset on each panel is the best-fit curve used for regression analysis.

ysis of a mutant retaining the C-terminal eight residues of NS1, to allow proper cleavage of the NS1/2A site, should help to clarify this matter.

While the nature of the processing event at the NS1/2A site remains obscure, we have been able to separate NS1 function from NS1-2A cleavage. It has been proposed that flavivirus NS1 may be associated with membranes via a glycosylphosphatidylinositol (GPI) anchor (45), implying that the NS1-2A cleavage is mediated via the proposed GPI transamidase (24). We have been unable to demonstrate biochemically the existence of a GPI anchor on YF NS1 (22). Nevertheless, if NS1 is indeed GPI anchored, expression of NS1 alone is predicted to ablate the signal for GPI anchoring (41). As demonstrated here, NS1 alone is sufficient for NS1 function in *trans*. It therefore seems unlikely that NS1-2A cleavage enables a posttranslational modification of NS1 required for NS1 function in *trans.*

Expression of NS1 was more efficient than NS1-2A in complementing YFΔSK, as seen by greater plaquing efficiency (Fig. 3) and earlier viral bursts (Fig. 5B). These observations could be related to the additional requirement for processing at the NS1-2A site or may be due to the regulation of NS1 function by NS2A. It is unlikely that exogenous expression of NS2A exerts a *trans*-dominant effect, as no difference in YF 17D growth was observed in BHK-SINrep21/NS1-2A. Of relevance is the observation that populations expressing NS1-2A were also less stable in plaquing efficiency than NS1-expressing pop-

ulations. Perhaps there is a selection against expression of NS2A alone or in combination with NS1 in BHK cells, leading to lower expression of functional NS1 on a per cell basis, although we have not measured this directly.

Previous genetic analyses provide compelling evidence that NS1 functions in RNA replication (26, 27). Viral RNA accumulation was impaired for viruses containing mutations of the first or both N-linked glycosylation sites of NS1 (27). Infection with a conditional mutant of NS1 under nonpermissive conditions also led to poor accumulation of viral RNA species (26). Upon shift of established infections from permissive to nonpermissive conditions, a greater defect was seen for minus-strand RNA accumulation than plus-strand RNA accumulation at the later stages of infection (18 to 36 h [26]). However, these previous studies were limited by the leaky phenotype of the mutant observed in shift-up experiments. Using the *trans*-complementation system described here, we were able to produce viruses lacking detectable NS1 function. This allowed us to examine viral RNA replication in the presence or absence of NS1. Furthermore, we focused attention on the detection and quantitation of very rare RNA species, permitting us to examine very early events in viral RNA replication. The results presented here thus extend previous observations of NS1 function to include the earliest observable events in RNA replication.

Flaviviruses are believed to replicate in the cytoplasm of infected cells in association with virus-induced membranes (5, 6, 20). RNA labeling kinetics at late times of infection suggest that RNA synthesis of Kunjin virus proceeds through a semiconservative but asymmetric replication cycle, wherein minus strands serve as template for multiple rounds of plus-strand synthesis (5). Recently, early events in RNA replication were examined for bovine viral diarrhea virus, a *Flaviviridae* family member of the genus *Pestivirus*. Plus and minus strands were both detectable by 4 h of infection, and the ratios of these species over time support a model of asymmetric replication (16).

The data presented here provide the first reported snapshots of early minus- and plus-strand synthesis during flavivirus replication. Analysis of each strand examined RNA accumulation initiated from 10^7 synchronized infections. We therefore infer that when equivalent numbers of minus strands have accumulated, each genome, on average, is in the process of completing its first minus strand. This time appears to be approximately 3 to 6 h for YF 17D and for complemented YFΔSK. Similar experiments confirm this time scale (data not shown). Importantly, within the first 21 h of infection, YFΔSK alone fails to achieve this level of minus strands. The simplest explanation for these results is that NS1 function is required either prior to or at the first cycle of minus-strand synthesis.

As noted in Fig. 6A and 7A, low levels of minus-strand RNA, which probably represent adsorption of residual RNA present in the inoculum, were detected at 10 min postinfection. We have detected large amounts of minus-strand RNA in our virus stocks, using the RPA described here (data not shown). These may be RNA molecules that were released from infected cells during virus growth, although we have not formally excluded the packaging of minus strands into YF particles. Given that the flavivirus entry process alone is estimated to take ≥30 min (15), it is highly unlikely that this minus-strand background was due to de novo RNA synthesis.

The infections analyzed for RNA replication are initiated by a large surplus of plus strands. Note that approximately 1×10^8 to 4×10^8 plus strands are associated with 10^7 PFU shortly after infection (Fig. 7B). It is not known whether this plus-strand excess reflects defective but packaged YF RNAs, inefficient steps in the infection process, naked RNAs in the inoculum, or some combination thereof. However, a 10-fold particle-to-infectivity ratio is consistent with that described for purified tick-borne encephalitis virus (7). By 3 h postinfection, 2×10^7 to 3×10^7 plus strands remain, which is very near the predicted number of input infectious genomes. The increase in replicating plus strands observed over the next 6 h is therefore consistent with the completion of first minus-strand synthesis and the early synthesis of additional plus strands. Only a steady decrease in plus strands is seen in noncomplemented YFΔSK, clearly suggesting a block prior to plus-strand synthesis and consistent with a role for NS1 in the earliest minus-strand synthesis.

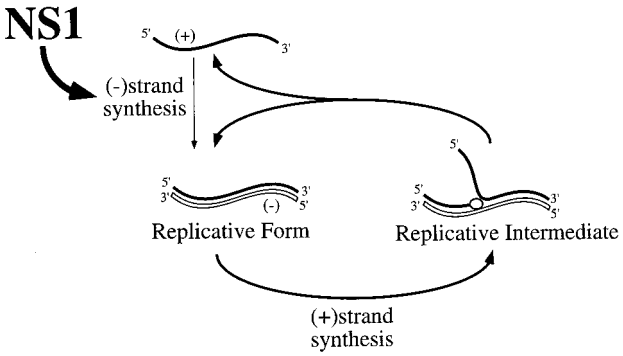

FIG. 8. Model illustrating our proposed role for NS1 in the flavivirus RNA replication cycle (based on reference 5).

Note that early plus- and minus-strand syntheses occur roughly in parallel, in contrast to the preferential accumulation of viral plus strands (50:1) described for late times of infection with YF (26). The ratio of plus strands to minus strands was calculated to be around 8:1 at 3 h (before the first complete cycle of minus-strand synthesis) and around 2:1 at 9 h (shortly after the first cycle of minus-strand synthesis) for YF 17D on BHK-SINrep21/GFP. This decrease in plus-strand-to-minus-strand ratio further supports our view that these represent the earliest minus strands, although it should be noted that both newly synthesized RNA molecules and input RNA molecules were measured. Furthermore, the asymmetry of plus-strand synthesis may increase over time, in accord with previous observations for YF (26) and bovine viral diarrhea virus (16).

Based on our data, we present a model (Fig. 8) in which NS1 is required for initial minus-strand synthesis. Previous data indicate that defects in NS1 also selectively block accumulation of minus strands late in infection (26). We cannot rule out a direct role for NS1 also in plus-strand synthesis, due to the interdependence of these replicative processes.

The precise function of NS1 in RNA replication remains to be identified. It seems curious that a nonstructural glycoprotein, topologically distinct from other replication components by its localization within vesicles, is essential for RNA replication. The early temporal requirement for NS1 suggests some interesting hypotheses. An organization model for NS1 function would implicate it in assembling the components of the viral replicase. This could be mediated through the relationship of NS1 and cellular membranes associated with replication, perhaps with NS1 inducing such structures. Additionally, NS1 may assemble replicase components via direct protein-protein interactions. A more mechanistic model might involve an unknown enzymatic function of NS1 or the regulation of another viral or host component through interaction with NS1. These possibilities are certainly not exclusive nor comprehensive. Nevertheless, *trans*-complementation should provide a

useful genetic tool with which to dissect NS1 as it pertains to RNA replication.

In summary, this work demonstrates that a YF genome defective in NS1 could be complemented by using noncytopathic Sindbis replicons to express NS1 in *trans*. We expect this technology to find broad utility in the study of RNA viruses, including other flaviviruses. Examination of YFΔSK provides strong evidence that NS1 functions prior to or at initial minus-strand synthesis.

ACKNOWLEDGMENTS

We thank Ricardo Galler and Arash Grakoui for early work on this project. We are also grateful to Eugene Agapov for helpful discussions during the course of this work and to Sean Amberg, Ilya Frolov, Scott McBride, Karen Reed, and Nicolas Ruggli for helpful discussions and critical reading of the manuscript.

This work was supported in part by Public Health Service grant AI31501.

REFERENCES

1. **Ausubel, F. M., R. Brent, R. E. Kingston, D. D. Moore, J. G. Seidman, J. A. Smith, and K. Struhl (ed.).** 1993. Current protocols in molecular biology. Greene Publishing Associates, New York, N.Y.
2. **Bredenbeek, P. J., I. Frolov, C. M. Rice, and S. Schlesinger.** 1993. Sindbis virus expression vectors: packaging of RNA replicons by using defective helper RNAs. J. Virol. **67:**6439–6446.
3. **Chambers, T. J., C. S. Hahn, R. Galler, and C. M. Rice.** 1990. Flavivirus genome organization, expression, and replication. Annu. Rev. Microbiol. **44:**649–688.
4. **Chambers, T. J., D. W. McCourt, and C. M. Rice.** 1990. Production of yellow fever virus proteins in infected cells: identification of discrete polyprotein species and analysis of cleavage kinetics using region-specific polyclonal antisera. Virology **177:**159–174.
5. **Chu, P. W. G., and E. G. Westaway.** 1985. Replication strategy of Kunjin virus: evidence for recycling role of replicative form RNA as template in semiconservative and asymmetric replication. Virology **140:**68–79.
6. **Chu, P. W. G., and E. G. Westaway.** 1992. Molecular and ultrastructural analysis of heavy membrane fractions associated with the replication of Kunjin virus RNA. Arch. Virol. **125:**177–191.
7. **Crooks, A. J., J. M. Lee, A. B. Dowsett, and J. R. Stephenson.** 1990. Purification and analysis of infectious virions and native non-structural antigens from cells infected with tick-borne encephalitis virus. J. Chromatogr. **502:** 59–68.
8. **Falgout, B., R. Chanock, and C.-J. Lai.** 1989. Proper processing of dengue virus nonstructural glycoprotein NS1 requires the N-terminal hydrophobic signal sequence and the downstream nonstructural protein NS2a. J. Virol. **63:**1852–1860.
9. **Falgout, B., and L. Markoff.** 1995. Evidence that flavivirus NS1-NS2A cleavage is mediated by a membrane-bound host protease in the endoplasmic reticulum. J. Virol. **69:**7232–7243.
10. **Frolov, I., E. A. Agapov, B. D. Lindenbach, B. M. Prágai, S. Schlesinger, and C. M. Rice.** 1997. Unpublished data.
11. **Frolov, I., T. A. Hoffman, B. M. Prágai, M. Lippa, S. Schlesinger, and C. M. Rice.** 1997. Unpublished data.
12. **Frolov, I., T. A. Hoffman, B. M. Prágai, S. A. Dryga, H. V. Huang, S. Schlesinger, and C. M. Rice.** 1996. Alphavirus-based expression systems: strategies and applications. Proc. Natl. Acad. Sci. USA **93:**11371–11377.
13. **Gaines, P. J., K. E. Olson, S. Higgs, A. M. Powers, B. J. Beaty, and C. D. Blair.** 1996. Pathogen-derived resistance to dengue type virus 2 in mosquito cells by expression of the premembrane coding region of the viral genome. J. Virol. **70:**2132–2137.
14. **Galler, R., A. Grakoui, and C. M. Rice.** Unpublished data.
15. **Gollins, S. W., and J. S. Porterfield.** 1985. Flavivirus infection enhancement in macrophages: an electron microscopic study of viral cellular entry. J. Gen. Virol. **66:**1969–1982.
16. **Gong, Y. H., R. Trowbridge, T. B. Macnaughton, E. G. Westaway, A. D. Shannon, and E. J. Gowans.** 1996. Characterization of RNA synthesis during a one-step growth curve and of the replication mechanism of bovine viral diarrhoea virus. J. Gen. Virol. **77:**2729–2736.
17. **Gorbalenya, A. E., A. P. Donchenko, E. V. Koonin, and V. M. Blinov.** 1989. N-terminal domains of putative helicases of flavi- and pestiviruses may be serine proteases. Nucleic Acids Res. **17:**3889–3897.
18. **Gorbalenya, A. E., E. V. Koonin, A. P. Donchenko, and V. M. Blinov.** 1989. Two related superfamilies of putative helicases involved in replication, recombination, repair and expression of DNA and RNA genomes. Nucleic Acids Res. **17:**4713–4730.
19. **Grakoui, A., and C. M. Rice.** Unpublished data.
20. **Grun, J. B., and M. A. Brinton.** 1988. Separation of functional West Nile virus replication complexes from intracellular membrane fragments. J. Gen. Virol. **69:**3121–3127.
21. **Haas, J., E.-C. Park, and B. Seed.** 1996. Codon usage limitation in the expression of HIV-1 envelope glycoprotein. Curr. Biol. **6:**315–324.
22. **Lindenbach, B. D., and C. M. Rice.** Unpublished data.
23. **Mackenzie, J. M., M. K. Jones, and P. R. Young.** 1996. Immunolocalization of the dengue virus nonstructural glycoprotein NS1 suggests a role in viral RNA replication. Virology **220:**232–240.
24. **Maxwell, S. E., S. Ramalingam, L. D. Gerber, L. Brink, and S. Udenfriend.** 1995. An active carbonyl formed during glycosylphosphatidylinositol addition to a protein is evidence of catalysis by a transamidase. J. Biol. Chem. **270:**19576–19582.
25. **Monath, T. P., and F. X. Heinz.** 1996. Flaviviruses, p. 961–1034. *In* B. N. Fields, D. M. Knipe, and P. M. Howley (ed.), Fields virology. Raven Press, New York, N.Y.
26. **Muylaert, I. R., R. Galler, and C. M. Rice.** 1997. Genetic analysis of yellow fever virus NS1 protein: identification of a temperature-sensitive mutation which blocks RNA accumulation. J. Virol. **71:**291–298.
27. **Muylaert, I. R., R. Galler, and C. M. Rice.** 1996. Mutagenesis of the N-linked glycosylation sites of the yellow fever virus NS1 protein: effects on virus replication and mouse neurovirulence. Virology **222:**159–168.
28. **Novak, J. E., and K. Kirkegaard.** 1991. Improved method for detecting poliovirus negative strands used to demonstrate specificity of positive-strand encapsidation and the ratio of positive to negative strands in infected cells. J. Virol. **65:**3384–3387.
29. **Olson, K. E., S. Higgs, P. J. Gaines, A. M. Powers, B. S. Davis, K. I. Kamrud, J. O. Carlson, C. D. Blair, and B. J. Beaty.** 1996. Genetically engineered resistance to dengue-2 virus transmission in mosquitoes. Science **272:**884–886.
30. **Pethel, M., B. Falgout, and C.-J. Lai.** 1992. Mutational analysis of the octapeptide sequence motif at the NS1-NS2A cleavage junction of dengue type 4 virus. J. Virol. **66:**7225–7231.
31. **Poch, O., I. Sauvaget, M. Delarue, and N. Tordo.** 1989. Identification of four conserved motifs among the RNA-dependent polymerase encoding elements. EMBO J. **8:**3867–3874.
32. **Preugschat, F., C.-W. Yao, and J. H. Strauss.** 1990. In vitro processing of dengue virus type 2 nonstructural proteins NS2A, NS2B, and NS3. J. Virol. **64:**4364–4374.
33. **Rice, C. M.** 1996. *Flaviviridae*: the viruses and their replication, p. 931–959. *In* B. N. Fields, D. M. Knipe, and P. M. Howley (ed.), Fields virology. Lippincott-Raven Publishers, Philadelphia, Pa.
34. **Rice, C. M., A. Grakoui, R. Galler, and T. J. Chambers.** 1989. Transcription of infectious yellow fever virus RNA from full-length cDNA templates produced by in vitro ligation. New Biol. **1:**285–296.
35. **Rice, C. M., E. M. Lenches, S. R. Eddy, S. J. Shin, R. L. Sheets, and J. H. Strauss.** 1985. Nucleotide sequence of yellow fever virus: implications for flavivirus gene expression and evolution. Science **229:**726–733.
36. **Sambrook, J., E. F. Fritsch, and T. Maniatis.** 1989. Molecular cloning: a laboratory manual. Cold Spring Harbor Laboratory, Cold Spring Harbor, N.Y.
37. **Schlesinger, J. J., M. W. Brandriss, and T. P. Monath.** 1983. Monoclonal antibodies distinguish between wild and vaccine strains of yellow fever virus by neutralization, hemagglutination inhibition, and immune precipitation of the virus envelope protein. Virology **125:**8–17.
38. **Smith, G. W., and P. J. Wright.** 1985. Synthesis of proteins and glycoproteins in dengue type 2 virus-infected Vero and *Aedes albopictus* cells. J. Gen. Virol. **66:**559–571.
39. **Strauss, J. H., and E. G. Strauss.** 1994. The alphaviruses: gene expression, replication, and evolution. Microbiol. Rev. **58:**491–562.
40. **Tan, B.-H., J. Fu, R. J. Sugrue, E.-H. Yap, Y.-C. Chan, and Y. H. Tan.** 1996. Recombinant dengue type 1 virus NS5 protein expressed in *Escherichia coli* exhibits RNA-dependent RNA polymerase activity. Virology **216:**317–325.
41. **Udenfriend, S., and K. Kodukula.** 1995. Prediction of omega site in nascent precursor of glycosylphosphatidylinositol protein. Methods Enzymol. **250:** 571–582.
42. **Wengler, G., G. Czaya, P. M. Färber, and J. H. Hegemann.** 1991. *In vitro* synthesis of West Nile virus proteins indicates that the amino-terminal segment of the NS3 protein contains the active centre of the protease which cleaves the viral polyprotein after multiple basic amino acids. J. Gen. Virol. **72:**851–858.
43. **Wengler, G., and G. Wengler.** 1991. The carboxy-terminal part of the NS3 protein of the West Nile flavivirus can be isolated as a soluble protein after proteolytic cleavage and represents an RNA-stimulated NTPase. Virology **184:**707–715.
44. **Wengler, G., and G. Wengler.** 1993. The NS 3 nonstructural protein of flaviviruses contains an RNA triphosphatase activity. Virology **197:**265–273.
45. **Winkler, G., S. E. Maxwell, C. Ruemmler, and V. Stollar.** 1989. Newly synthesized dengue-2 virus nonstructural protein NS1 is a soluble protein but becomes partially hydrophobic and membrane-associated after dimerization. Virology **171:**302–305.
46. **Winkler, G., V. B. Randolph, G. R. Cleaves, T. E. Ryan, and V. Stollar.** 1988. Evidence that the mature form of the flavivirus nonstructural protein NS1 is a dimer. Virology **162:**187–196.